Digital Twin based Implementation of Active Traction Substation in DC Railway Systems

Hamed Jafari Kaleybar
Energy Department
Politecnico di Milano
Milano, Italy
hamed.jafari@polimi.it

Morris Brenna
Energy Department
Politecnico di Milano
Milano, Italy
morris.brenna@polimi.it

Luca Pugi
Dept. of Industrial Engineering
University of Florence
Florence, Italy
luca.pugi@unifi.it

Luca di Carlo
Dept. of Industrial Engineering
University of Florence
Florence, Italy
luca.dicarlo@unifi.it

Aljon Kociu
Dept. of Industrial Engineering
University of Florence
Florence, Italy
aljon.kociu@unifi.it

Massimo Delogu
Dept. of Industrial Engineering
University of Florence
Florence, Italy
massimo.delogu@unifi.it

***Abstract*—Electric railway systems (ERS), stand as a pivotal technology in the transportation sector. Given the extensive nature of these networks, conducting precise simulations becomes imperative for ensuring dependable and safe operations aligned with real-world performance. Meanwhile, the development of more eco-friendly sections with increased energy efficiency have become a goal for ERSs which are one of the high-consumption users for grid. Focusing on regenerative braking energy (RBE), this paper addresses the potential of bidirectional traction substations known as active traction substation (ATSS) with interleaved PWM rectifiers, allowing bidirectional power flow and promoting RBE revert to the main grid. In this paper, an approach is presented to develop a digital twin (DT) concept of bilateral DC railway system with ATSS which allows to receive the real data from physical system and estimate the transient events and power quality issues. Utilizing the current setup of the Italian 3 kV DC railway line as a real-world example, the study assesses different substation characteristics to pinpoint the optimal design, considering essential metrics like voltage ripple, stress on passive components, total harmonic distortion, voltage and current imbalances, and achieving unity power factor operation. Due to the inclusion of a real case study, the findings accurately reflect real-world parameters.**

Keywords—Active traction substation, regenerative braking energy, PWM rectifier, digital twin, railway.

I. Introduction

Aligned with the obligations outlined by the EU's climate targets, achieving zero-carbon transportation systems by 2050 marks a significant stride for the transportation sector [1]. Consequently, there is a growing interest in innovative solutions to enhance energy efficiency within electric railway systems. A considerable body of research is dedicated to exploring the potential of regenerative braking energy (RBE) utilization [2]. Regenerative braking was first introduced in electric railway systems (ERSs) with the advent of DC chopper systems in the 1970s. Initially, it was implemented primarily in tramways and metro systems as an enhancement over existing dissipative electric braking technology. This early adoption of regenerative braking in railways was driven by the inherent characteristics of railway technology, such as reduced motion resistances and high loading capacity, enabling the transportation of heavy masses with minimal power consumption. However, in conventional railway systems, recovered energy cannot be stored and must be transferred through the catenary to another load, typically another train on the same line. If there is no train in adjacent, the RBE is wasted in onboard rheostats. Meanwhile, to maximize the coincidence of braking train and traction train, scheduling and timetables are useful methods to optimize and ensure a balanced distribution of maneuvers along the line, maximizing energy recovery and system efficiency [3, 4]. However, there exist significant portion of recoverable RBE even with optimizing methods. Different solutions have been proposed in recent studies to utilize these dissipated portions of RBE. Despite the additional costs associated with energy storage systems (ESS), they are known as one of promising solutions [5, 6]. In this regards, incorporating both onboard and stationary ESSs, which utilize various electric storage mediums like supercapacitors, batteries, or flywheels, represents contemporary approaches to harnessing regenerative braking energy within DC railway systems.

In line with reducing energy wastage and minimizing the need for external storage systems, leading to cost savings and simplifying the overall infrastructure, an alternative is taking advantage of bidirectional/reversible traction substations [7-9]. In last years, many research are carried out on the topic of reversible substations focusing on the possibilities of integrating the existing diode-based multi-pulse rectifier traction power substation (TPSS) with an antiparallel inverter or even replacing diode-based multi-pulse rectifier by a controlled thyristor rectifier [10]. Different method in this context are explained in details in [11, 12].

Considering the advantages of PWM rectifiers in comparison to traditional rectifiers [13], their performance in TPSSs are evident in terms of higher efficiency, improved power quality, enhanced dynamic response, reduced size and weight, as well as greater flexibility and adaptability. These advantages make PWM rectifiers a preferred choice for modern railway traction systems, offering superior performance and reliability compared to reversible substations with parallel inverters and diode rectifiers or thyristor rectifiers [14]. Replacing existing traditional diode-based TPSSs with such innovative technology necessitates thorough pre-study, detailed modeling, and simulations based on real data. This ensures precise sizing and design of TPSS and associated equipment while retaining existing parameters and features to minimize costs.

This study was carried out within the MOST – Sustainable Mobility National Research Center and received funding from the European Union Next-Generation EU (PIANO NAZIONALE DI RIPRESA E RESILIENZA (PNRR) – MISSIONE 4 COMPONENTE 2, INVESTIMENTO 1.4 – D.D. 1033 17/06/2022, CN00000023). This manuscript reflects only the authors' views and opinions, neither the European Union nor the European Commission can be considered responsible for them.

2024 IEEE International Conference on Environment and Electrical Engineering and 2024 IEEE Industrial and Commercial Power Systems Europe (EEEIC / I&CPS Europe) | 979-8-3503-5518-5/24/$31.00 ©2024 IEEE | DOI: 10.1109/EEEIC/ICPSEUROPE61470.2024.10751526

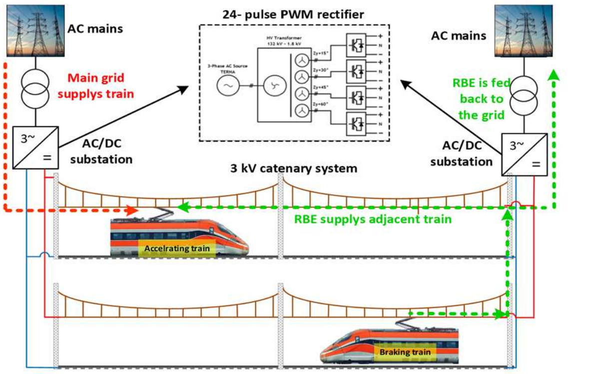

Fig. 1. General configuration of the under-study bilateral 3 kV railway system.

In this regard, on of the main promising solutions is to develop a model based Digital Twin (DT) of real physical systems and test the different scenarios with such a model. Even the implementation of DT for ERSs are studied in literature for some parts [15-18], the application of this method to the modern ATSS is not discussed yet. Accordingly, in this paper, an approach is presented to develop a DT concept of bilateral DC railway system with ATSS which allows to receive the real data including line data, train positions, traffic situations and etc. from physical system and estimate the transient events and power quality issues together with analysis of peak powers, voltage drops. Utilizing the existing network of the Italian 3 kV DC railway line as a real case study, the study assesses different substation characteristics and loading scenarios to pinpoint the optimal design, considering essential metrics.

In the subsequent sections, the paper unfolds as follows. Section II elucidates the operational principles of under study bilateral ERS with ATSS. Following this, Section III delves into proposed control strategy. A comprehensive case study based simulations are undertaken in Section IV. Lastly, Section V encapsulates the concluding remarks of the paper.

II. Principles of Under Study System

The general structure of under study 3 kV ERS is shown in Fig. 1. It includes sections between two consecutive TPSS implemented as a bilateral power supply of a DC railway line, by the shunt connection of two identical TPSS. The main different sections of the structure includes HV primary-side, ATSS, overhead catenary line (OCL) and trains.

A. Proposed ATSS and Primary-Side HV Grid

The existing AC/DC conversion system in Italian 3 kV DC ERSs employs multi-pulse diode-bridge traditional rectifiers with the average distance of 15 km between each TPSS. Accordingly, the implementation of proposed ATSS is considered in the same location assuming the replacement of traditional AC/DC conversion with PWM rectifiers.

The proposed ATSSs are connected to the AC grid in primary-side to the Italian suburban area which is mostly based on 132 kV medium voltage (MV). Although the short length and voltage level permit a purely RL series line model, a T-model is utilized to accommodate the line capacitance. A multi-pulse step-down transformer based on zig-zag connection in primary-side is positioned at TPSS to adjust the grid voltage for the conversion process. Each secondary winding, supplies a separate PWM rectifier based on three-level neutral point-clamped (3L-NPC) type which behave as four quadrant converters (4QCs). The phase shift in secondary-side Y connections are considered 15° which realize 24-pulses in output DC voltage. The nominal voltage of line is considered as 3.6 kV in the positions of ATSS with possibility of 20% overvoltage due to the related standards in ERS. Meanwhile, minimum operating voltage is set to 2.4 kV. Regarding suitable PWM converter operation, the primary-side AC voltage should be less than the DC-side voltage. Accordingly, the secondary-side voltage of transformers are set to 1.7 kV.

All ATSS's PWM converters are sized based on the existing TPSS's power range for a 5.4 MW is consistent with the standard nominal powers commonly observed in Italian AC/DC conversion groups. To decrease and smooth the output DC voltage ripples, DC-link capacitors are implemented at the 4QCs output. Furthermore, inductor branches are positioned upstream of each converter to facilitate the linear operation of the rectifier. This assumes that the series inductance of the transformer alone may not be adequate to charge the DC-link capacitor at a higher voltage.

B. Overhead Catenary Line (OCL) Modelling

The performance of the OCL in DC lines has undergone significant advancements over time. Initially, contact lines comprised a single copper messenger wire with a cross-section of 120 mm^2, fixed anchoring, and mechanical tension of about 1075 N, alongside two contact wires with a regulated cross-section of 100 mm^2 adjusted to 750 N each [19]. The total cross-section of this configuration was 320 mm^2. As train speeds increased to 150 km/h, improving the quality of the OCS and refining the interaction between the train pantograph and catenary became paramount.

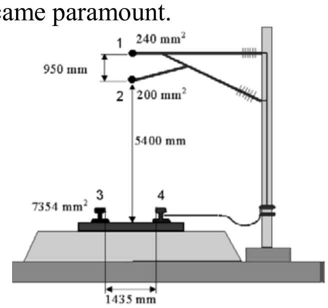

Fig. 2. The Italian 3 kV DC OCL conductors geometries [19].

To adapt to these changes, the four power supply windings of the 4QCs are now utilized as independent switching inductances of the step-down chopper by short-circuiting the primary side of the transformer. Consequently, an additional messenger wire was introduced, and mechanical tension was increased. This new configuration featured a total cross-section of 440 mm^2, with a mechanical tension of 1375 N for the messenger wire and 1000 N for the contact wires. This enhanced design proved to be highly effective and was subsequently implemented on lines with a maximum speed of 250 km/h, forming the basis of Italian 3 kV DC high-speed lines. As traffic increased and nominal rating values rose, further improvements to OCL wires were implemented. Table I presents various structures designed for the 3 kV DC system. Furthermore, the OCL resistance, along with the running rails resistance (acting as the return path for the current), is collectively treated as a unified resistance in series with an inductance, meticulously modeled as lumped parameters.

TABLE I. STANDARDS FEATURES OF 3 KV DC ERS OCL CONDUCTOR [19].

Characteristics of railway lines		Contact line	Messenger wires			Contact wires		
Maximum speed (km/h)	Intensity of traffic	Copper wire section (mm^2)	Number	Section (mm^2)	Mechanical tension (N)	Number	Section (mm^2)	Mechanical tension (N)
200	Low	320	1	120	1375	2	100	1000
200	Mean	440	2	120	1125	2	100	1000
200	High	610	2	155	1000	2	150	1125
250	Mean	540	2	120	1500	2	150	1875
250	High	610	2	155	1625	2	150	1875

The incorporation of the inductance aims not only to accurately depict DC transient voltage events but also to address potential interference caused by the contact line to nearby equipment. Building upon the methodology elucidated in [20], an EMU shunt capacitor of 1 mF is meticulously factored into the equation. The contact line resistance and inductance are meticulously modeled with per-unit length values of 0.057 Ω/km and 1.2 mH per km, respectively. Under this meticulous scheme, the slope of traction transient currents is decisively restricted to a mere 20 kA/s, while the slope of traction to regenerative braking transients is meticulously capped at 10 kA/s. Such meticulous limitations ensure the contact line voltage remains well below a stringent safety threshold of 4 kV, promptly activating EMU protection devices should this threshold be exceeded.

C. Train Motion Modelling

To effectively simulate the dynamic movements of trains for accurate analysis ATSS and it's control method, it's imperative to account for all the forces acting upon them, encompassing tractive forces, resistance, gradients, and the effort/speed curve. By thoroughly considering these forces during train motion, and using Newton's second law, the train motion equation can be expressed as:

$$\sum F = F_{Tr} - F_{grad} - F_{drag} = a \times M_{eff} \tag{1}$$

Where Meff is the equivalent mass and a is the train acceleration. The tractive effort (F_{Tr}) is a total tractive force. The drag force (F_{drag}) which can be calculated by Davis equation and train data sheet information is applied for load torque calculation as:

$$F_{drag} = a + bv + cv^2 \tag{2}$$

Meanwhile, the gradient force and curve force can be derived as:

$$F_{grad} = M_{eff} \times g \times sin\theta \tag{3}$$

In order to calculate train power according to the total force and speed of train, the following equation can be used. Which η is train efficiency and P_{aux} is the consumed auxiliary internal power of train.

$$P_{\text{train}} = \frac{F \times v}{\eta} + P_{aux} \tag{4}$$

At first, the input data including line, train and utilization data are obtained by DT based model as shown in Fig. 3 and train movement equations are calculated. Then based on the TPSS specification, track arrangement and conductance, the number of nodes and matrices are created and finally, the power flow analysis and voltage drops calculation can be carried out.

Rome-Florence double track railway line is selected as a case study. The line also known as the "Direttissima" covers a distance of 253.6 km and was built alongside a significant portion of Italy's historical and cultural landscape. The maximum slope is 8% while the minimum radius of the curves are equal to 3000 meters. consists of a double track with a track gauge of 1435 mm and an interbinary track of 4 m to neutralize the dynamic effects of trains during crossings. The tracks are armed with Vignoles UNI 60 E1 rails that are electrically welded for durability and smooth operation. The maximum design speed for trains on this line is 250 km/h, emphasizing its focus on high-speed travel. The contact line along the entire Rome-Florence double-track railway line is homogeneous. The positions and arrangements of substations together with measured slope for all distance of the line are illustrated in Fig. 4. The line is powered by a total of 18 traction substations strategically located along the route with average distance of 15 km between each TPSS. These substations play a crucial role in supplying the necessary electrical power to the trains for propulsion, lighting, and other onboard systems.

ETR 500 and 1000 trains which are mostly travel in this line are considered as selected locomotive for modeling with dedicated information with maximum power of 9 MW in AC line and 7.2 MW in DC lines.

III. PROPOSED CONTROL SYSTEM FOR BIDIRECTIONAL ATSS

The chosen modulation method for controlling each 3L-NPC of ATSS in this study is PWM based voltage-oriented control (VOC) method. This decision is based on the bidirectional characteristics of the three-level converters and the objective to operate at unity power factor with minimal current harmonics. Various techniques have been introduced for PWM rectifier control over the past few decades, broadly categorized into four families: voltage-oriented control (VOC), voltage-based direct power control, virtual-flux oriented control, and virtual-flux based direct power control VF-DPC.

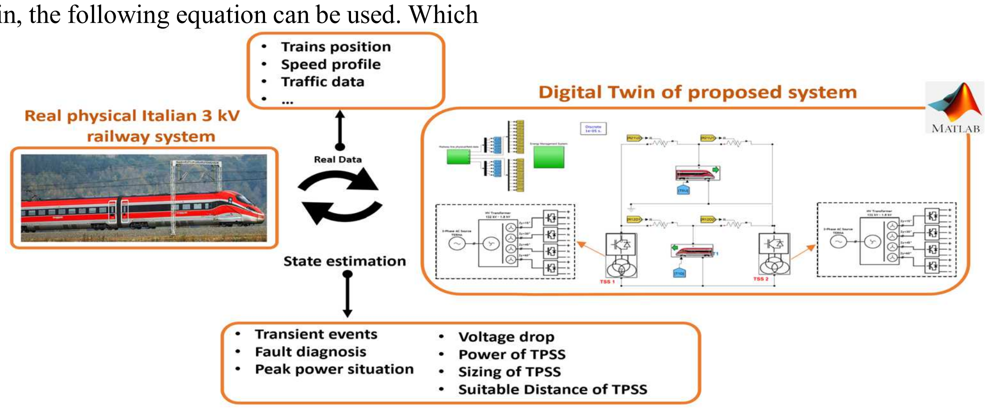

Fig. 3. Proposed model-based DT implemneted in Matlab/Simulink platform.

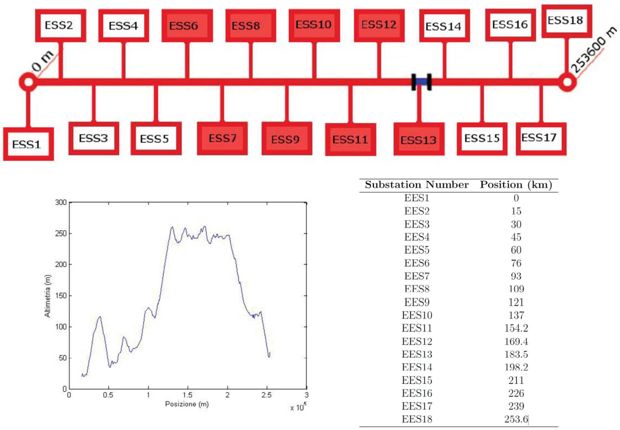

Substation Number	Position (km)
EES1	0
EES2	15
EES3	30
EES4	45
EES5	60
EES6	76
EES7	93
EES8	109
EES9	121
EES10	137
EES11	154.2
EES12	169.4
EES13	183.5
EES14	198.2
EES15	211
EES16	226
EES17	239
EES18	253.6

Fig. 4. Rome-Florence TPSS location and positions with line slope.

These control methods conceptualize the converter as an AC rotating machine with its rotating flux, making it easier to manipulate using PI regulators. While all control types adhere to a DC voltage reference, oriented controls directly follow current references, whereas direct power controls (DPC) track P and Q powers.

Due to the significant advantages of VOC including precise control of voltage and current, allowing for efficient operation at unity power factor with minimal current harmonics, simplifying the tuning of PI regulators and offering greater stability, it is preferred for achieving high-performance operation in proposed study.

Applying the KVL for each NPC converter and decoupling voltages and currents into d-q parts, the following components can be extracted as (5) to (7) [21, 22].

$$V_{cd} = -(L_g s+R_g)i_d + L_g \omega i_q + V_{gd} \tag{5}$$

$$V_{cq} = -(L_g s+R_g)i_q - L_g \omega i_d + V_{gq} \tag{6}$$

$$\begin{bmatrix} V_{cd} \\ V_{cq} \end{bmatrix} = \begin{bmatrix} -(L_g s+R_g) & \omega L_g \\ -\omega L_g & -(L_g s+R_g) \end{bmatrix} \begin{bmatrix} i_d \\ i_q \end{bmatrix} + \begin{bmatrix} V_{gd} \\ V_{gq} \end{bmatrix} \tag{7}$$

The overall control scheme depicted in Fig. 5 follows the outlined control procedure detailed in equations (5) and (6). The calculation of the angle ωt integrates a PLL block, which can also monitor the grid frequency if required. Managing two four-level rectifiers, the measured grid current comprises the summation of currents upstream of the inductances, resulting in a total of 24 output pulses, from the PWM modulation. V_{dc} voltage is measured via the two capacitances, bypassing the neutral point. Opting for actual values instead of reference ones for the feed-forward terms assumes that signals aren't excessively noisy, as their noise impacts control voltages. While filtering measurements can reduce noise, it introduces delay, potentially affecting performance during high transients. Utilizing four converters offers advantages in redundancy, power distribution across devices, and the implementation of interleaved converters. Interleaving involves shifting carrier signals between bridges, nullifying high-frequency components in both grid and DC voltages. For a system with N converters in series or parallel, the necessary phase shift, assuming a consistent switching frequency, corresponds to "$2\pi/N$" radians. Hence, for $N=4$ converters, the appropriate phase shift 90°.

IV. Simulation Results

The proposed ERSs including ATSS employing VOC method is implemented using MATLAB/SIMULINK with the possibility of updating input data based on real data. The considered parameters are detailed in Table II. In order to test more real conditions and measure the stress on ATSS accurately based on real situation, the simulation covers a full traction cycle of a locomotive, encompassing phases of acceleration, cruising, and braking.

TABLE II. Simulation Parameters

Parameter	***Value***
Primary side voltage	132 kV
Grid frequency	50 Hz
Transmission line series resistance	0.18 Ω
Transmission line series inductance	0.65 mH
Transmission line shunt capacitance	1.50 μF
Nominal power transformer of ATSS	6 MVA
Secondary side voltage	1.6 kV
Secondary side inductance	1 mH
NPC DC-link capacitance	50 mF
IGBT Switching frequency	1250 Hz
OCL resistance	0.057 Ω
OCL inductance	1.2 mH

Due to the relatively higher switching frequency of converters inside ATSS, the sampling time is set to 20 μs and accordingly two consecutive ATSS with 15 km distance are simulated considering different scenarios of loading and train positions. To simulate exactly time-varying OCL resistance, variable resistance are implemented which varies based on the position trains. The main goal of analysis is the evaluation of ATSS performance based on interleaved 3L-NPC converters and from a power quality phenomena point of view. Figure 5. shows the information about selected route including slope and possible timetable with high traffic conditions. Meanwhile, Fig. 5.c illustrates the power consumption of ETR1000 train in this route with almost 6.4 MW peak in acceleration mode. Due to the line limitations, the maximum speed of train is considered to 160 km/h for this route.

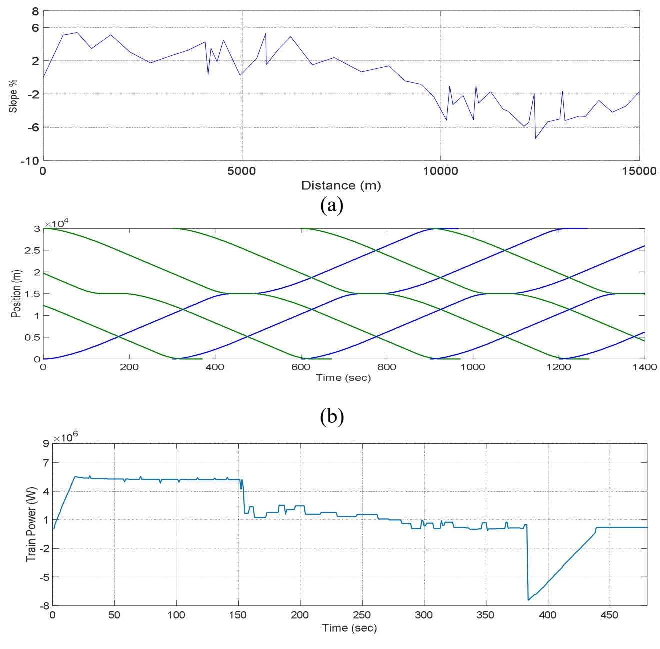

Fig. 5. Case study data. a) line slope, b) Timetable, c) Train power in full cycle.

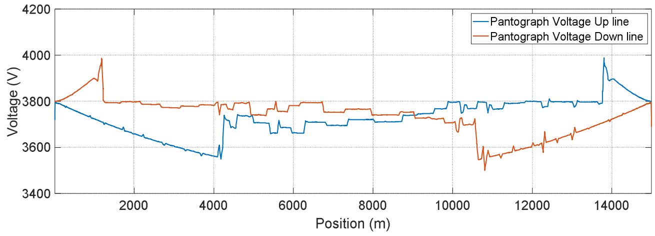

Fig. 6. Pantograph voltage in up-and down tracks.

In Figure 6 are shown the pantograph voltage of trains in both up-track and down-track. The position of ATSS1 is considered in 0 and the position of ATSS2 is considered in 15 km. First of all, it can be observed that the pantograph voltage both are kept around the 3800 V at their respective DC busbars, the transient voltage relies on the contact line properties, and in turn, on the distance from the substation. The maximum voltage drop points and voltage increases are dedicated to the acceleration and braking mode of trains which are close to the substations. The voltage increases in braking phases are regarding the sharp braking and rescaling of simulation, which in this case is not restricted to a mere 20 kA/s and its higher than this value. However, it can be seen that also for such a high current transients thanks to the PWM rectifier, the contact line voltage remains well below a stringent safety threshold of 4 kV. The output rectified DC voltage of ATSSs shown in Fig. 7 reveal this performance and high regulation features. It can be seen that the maximum voltage ripples happen in braking modes where it is less than 80 volt (3%). This capability confirms that the possible distance of ATSSs can be considered also more than 15 km.

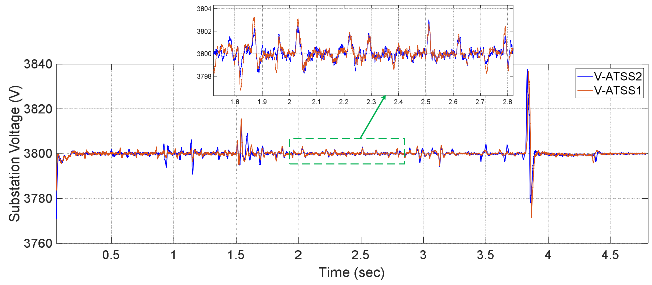

Fig. 7. Rectified voltage of ATSSs.

In Figure 8 are shown the capacitor voltages for one of the interleaved 3L-NPCs. It is noticeable that the proposed control method based on VOC and PWM keeps the voltages closer to reference value of 1900 V, due to the higher overall capacitance from each busbar to the NP.

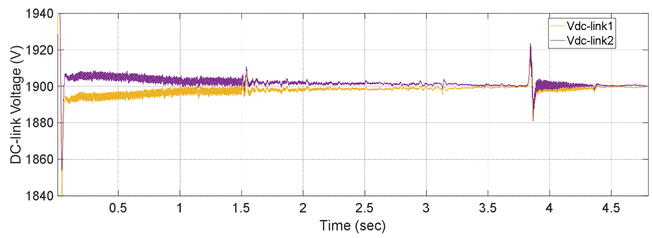

Fig. 8. DC-Link voltage capacitors in interleaved converter.

In Figure 9 is shown the active and reactive powers at the PCC point of ATSS 1, with the corresponding power factor calculation. It is obvious that the reactive power of grid is almost kept around zero which addresses the performance of PWM rectifiers in power factor correction. The active power absorbed from grid is a little bit higher than train power which corresponds to the power loss at the conversion and line copper losses.

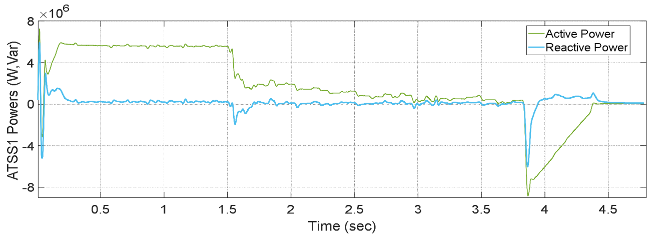

Fig. 9. Active and reactive powers of ATSS 1.

In Figure 10 are shown the three-phase current of ATSS 1 together with FFT analysis for two traction and braking phases. It can be seen that the current amplitude is different, comprising acceleration, cruising and braking phases and for all cycles they are almost sinusoidal.

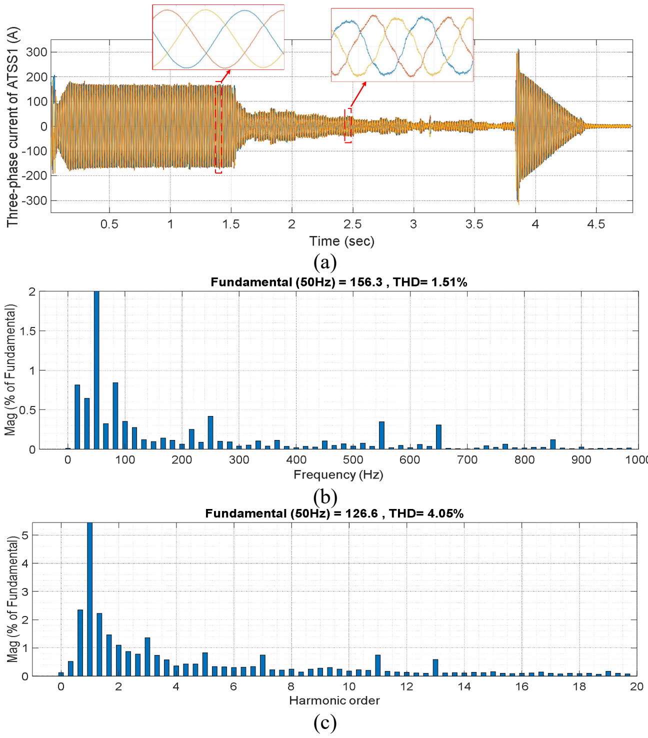

Fig. 10. Three-phase currents and FFT analysis. a) Three-phase currents in Primary side of ATSS1. b) FFT analysis in traction mode. c) FFT analysis in acceleration mode.

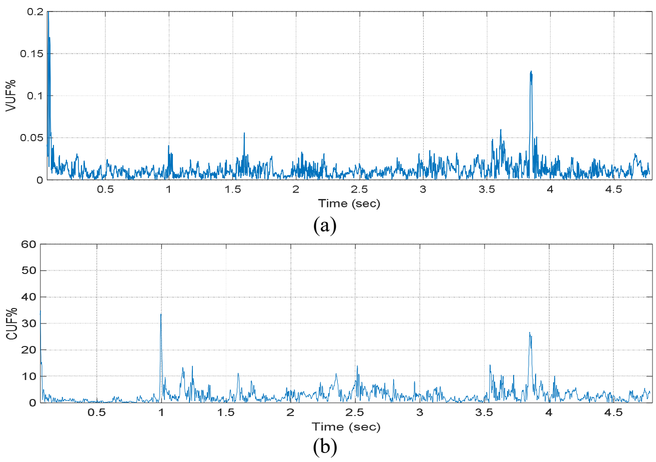

Fig. 11. Voltage and current unbalance ratioes in primary side of ATSS1.

A comparison of Fig. 10.b and Fig. 10.c, reveal that the current at braking mode has higher low order harmonics contents, that increases the THDs in average 4% for higher currents and almost 10% for lower currents. However, THD% of voltages are kept below standard values for all scenarios. To analyze the unbalanced ratio of currents and voltage at PCC, voltage unbalanced factor percentage (VUF%) and current unbalanced factor percentage (CUF%) as a ratio of negative sequence to positive sequence are measured as Fig.11. It is obvious that even for higher transients currents, VUF% and CUF% are consecutively less than 0.15% and 30% and remains consistently below standard values across all scenarios.

V. CONCLUSIONS

In this study, the design and digital-twin based simulation of an advanced 4QC-based active traction substation were developed, for the 3 kV Italian railway system configuration. The 24-pulse based configuration based on zig-zag transformers and interleaved 3L-NPC based structures are developed. The presented approach aimed to develop a digital twin concept of bilateral DC railway system with ATSS which allows to receive the real data including line data, train positions, traffic situations and etc. from physical system and estimate the transient events and power quality issues together with analysis of peak powers, voltage drops. Accordingly, a real load model considering a time-rescaled equivalent complete traction cycle is simulated based on ETR trains. It has been found that the developed model has superior performances in terms of transient times at initialization, voltage ripple at steady state, capacitor stresses due to voltage unbalance at DC bus, harmonic cancellation due to interleaving operation, and voltage and current THDs for all traction and braking phases. Having more DC-link capacitors of the same size, and sharing the stress to interleaved converters, implies that the voltage at steady state presents lower ripple of double grid frequency, and therefore that the voltage oscillation measured at each capacitor remains within a narrower interval. In conclusion, interleaved PWM rectifiers based TPSS are preferred, due to the proven advantages to be a promising solution for replacing traditional diode based TPSS. Furthermore, it is revealed that replacing these traditional TPSS with PWM based ATSS, can give the opportunity to increase the distance of substations.

REFERENCES

[1] Plötz, P., Wachsmuth, J., Gnann, T., Neuner, F., Speth, D. and Link, S., 2021. Net-Zero-Carbon Transport in Europe until 2050—Targets, Technologies and Policies for a Long-Term EU Strategy. *Karlsruhe: Fraunhofer Institute for Systems and Innovation Research ISI.*

[2] Ceraolo, M., Lutzemberger, G., Frilli, A., Pugi, L. Regenerative braking in high speed railway applications: Analysis by different simulation tools (2016) *EEEIC 2016 – Int. Conference on Environment and Electrical Engineering*, art. no. 7555474.

[3] H. J. Kaleybar, M. Davoodi, M. Brenna and D. Zaninelli, "Applications of Genetic Algorithm and Its Variants in Rail Vehicle Systems: A Bibliometric Analysis and Comprehensive Review," in *IEEE Access*, vol. 11, pp. 68972-68993, 2023, doi: 10.1109/ACCESS.2023.3292790.

[4] Sun, P., Zhang, C., Jin, B., Wang, Q. and Geng, H., 2023. Timetable optimization for maximization of regenerative braking energy utilization in traction network of urban rail transit. *Computers & Industrial Engineering*, *183*, p.109448.

[5] Khodaparastan, M., Mohamed, A.A. and Brandauer, W., 2019. Recuperation of regenerative braking energy in electric rail transit systems. IEEE Transactions on Intelligent Transportation Systems, 20(8), pp.2831-2847.

[6] Ghaviha, N., Campillo, J., Bohlin, M. and Dahlquist, E., 2017. Review of application of energy storage devices in railway transportation. *Energy Procedia*, *105*, pp.4561-4568.

[7] Fan, F., Li, Y., Ziani, S. and Stewart, B.G., 2021, February. Reversible substation modelling with regenerative braking in DC traction power supply systems. In *2021 IEEE Texas Power and Energy Conference (TPEC)* (pp. 1-6).

[8] F. Hao, G. Zhang, J. Chen, Z. Liu, D. Xu and Y. Wang, "Optimal Voltage Regulation and Power Sharing in Traction Power Systems With Reversible Converters," in *IEEE Transactions on Power Systems*, vol. 35, no. 4, pp. 2726-2735, July 2020.

[9] M. Popescu, A. Bitoleanu, V. Suru and A. Preda, "System for converting the DC traction substations into active substations," *2015 9th Int. ATEE.)*, Bucharest, Romania, 2015, pp. 632-637, doi: 10.1109/ATEE.2015.7133893.

[10] V. Gelman, "Insulated-Gate Bipolar Transistor Rectifiers: Why They Are Not Used in Traction Power Substations," in *IEEE Vehicular Technology Magazine*, vol. 9, no. 3, pp. 86-93, Sept. 2014.

[11] Popescu, M. and Bitoleanu, A., 2019. A review of the energy efficiency improvement in DC railway systems. *Energies*, *12*(6), p.1092.

[12] H. Jafari Kaleybar, M. Brenna and L. Pugi, "Reversible Traction Substations in DC Railway Systems: A Comparative Study of Approaches," *2023 IEEE EEEIC / I&CPS Europe*, Madrid, Spain, 2023, pp. 1-6.

[13] Rodríguez, José R., Juan W. Dixon, José R. Espinoza, Jorge Pontt, and Pablo Lezana. "PWM regenerative rectifiers: State of the art." *IEEE Transactions on Industrial Electronics* 52, no. 1 (2005): 5-22.

[14] Wang, Lei, Gang Zhang, Maosheng Shen, Hengli Quan, and Zhigang Liu. "A novel traction supply system for urban rail transportation with bidirectional power flow and based on PWM rectifier." In IEEE *2009 international conference on energy and environment technology*, vol. 2, pp. 40-43.

[15] M. Ahmadi, H. J. Kaleybar, M. Brenna, F. Castelli-Dezza and M. S. Carmeli, "Adapting Digital Twin Technology in Electric Railway Power Systems," *2021 12th Power Electronics, Drive Systems, and Technologies Conference (PEDSTC)*, Tabriz, Iran, 2021, pp. 1-6.

[16] Gao, Y., Qian, S., Li, Z., Wang, P., Wang, F. and He, Q., 2021, July. Digital twin and its application in transportation infrastructure. In *2021 IEEE 1st International Conference on Digital Twins and Parallel Intelligence (DTPI)* (pp. 298-301).

[17] S. Ghaboura, R. Ferdousi, F. Laamarti, C. Yang and A. E. Saddik, "Digital Twin for Railway: A Comprehensive Survey," in *IEEE Access*, vol. 11, pp. 120237-120257, 2023.

[18] L. Pugi, M. Brenna, M. Delogu, L. di Carlo and H. J. Kaleybar, "An Integrated Platform for the Simulation of Multimodal Trains on Discontinuosly Electrified Lines," *2023 IEEE Vehicle Power and Propulsion Conference (VPPC)*, Milan, Italy, 2023, pp. 1-6.

[19] H. J. Kaleybar, M. Brenna and F. Foiadelli, "Compatibility of Present 3 kV DC and 2×25 kV AC High-Speed Railway Power Supply Systems Towards Future MVDC System," IEEE *12th .PEDSTC*, Tabriz, Iran, 2021, pp. 1-6.

[20] Torabi Jafrodi S, Ghanbari M, Mahmoudian M, Najafi A, M. G. Rodrigues E, Pouresmaeil E. A Novel Control Strategy to Active Power Filter with Load Voltage Support Considering Current Harmonic Compensation. *Applied Sciences*. 2020; 10(5):1664. https://doi.org/10.3390/app10051664.

[21] M. Malinowski, M. Jasinski, and M. P. Kazmierkowski, “Simple direct power control of three-phase PWM rectifier using space-vector modulation (DPC-SVM),” IEEE Transactions on Industrial Electronics, vol. 51, no. 2, pp. 447–454, 2004.

[22] I. M. G. Llaneza, H. J. Kaleybar and M. Brenna, "Implementation of Active Power Substation for Harvesting Regenerative Braking Energy in Italian 3 kV Railway Systems," *2023 AEIT International Annual Conference (AEIT)*, Rome, Italy, 2023, pp. 1-6.